Nanoparticles

DOI: 10.1002/anie.200903864

Making Use of Bond Strength and Steric Hindrance in Nanoscale "Synthesis"**

*Yanhu Wei, Kyle J. M. Bishop, Jiwon Kim, Siowling Soh, and Bartosz A. Grzybowski**

With the focus of nanotechnology gradually shifting from individual nanoobjects to larger assemblies[1,2] and materials,[3,4] new methods are needed to "bond" nanoscale components through specific and directional interactions.[5,6] Unlike in chemistry, however, where bond specificity and directionality are inherent to atoms of different types, nanoscopic objects interact through highly symmetric interaction potentials (e.g., electrostatic,[3] van der Waals,[7] dipole–dipole,[8] hydrogen bonding,[9] etc.) and typically assemble into bulk, three-dimensional aggregates[8,10] or crystals.[3,8,11] To date, methods of directional bonding/assembly at the nanoscale have been limited to either the use of already directional organic templates (DNA,[12–14] proteins,[15,16] small molecules[17]) or the formation of topological defects at the "poles" of metal nanoparticles[6,18,19] or nanorods[20,21] which then assemble into short, linear oligomers. Here, we demonstrate that the toolbox of "nanosynthesis" can be significantly enhanced by extending the all-important chemical concepts of bond strength and steric hindrance to the nanoscale. Specifically, using a system of two-component Au/Fe_3O_4 nanoparticles (NPs),[22,23] we show that the combination of bond strength due to the cross-linking of Au domains and steric hindrance due to the bulky Fe_3O_4 parts can drive and control nanoscale "reactions" leading to dimeric, trimeric, tetrameric, and oligomeric structures (primitive "nanomolecules"). These reactions can progress with high selectivities and yields, and with reactivity trends analogous to those seen in molecular-scale metal–ligand complexes (Figure 1a and Ref. [24]). The progress and outcomes of the nanoscale transformations are described by a statistical mechanical model which quantifies the free energies of nanoscale "bonding" and is applicable to other types of systems of "reactive" nanoparticles, including those based on DNA interactions.[13,25]

Our experiments were based on composite Fe_3O_4/Au NPs (Figure 1b) comprising smaller Au (radius varied controllably for $R_1 = (3 \pm 0.3)$ nm to $R_1 = (7.3 \pm 1.7)$ nm; standard deviation, $\sigma = 11$–$23\,\%$) and larger Fe_3O_4 domains ($R_2 = (11.8 \pm 1.0)$ nm to $R_2 = (17.5 \pm 2.3)$ nm; $\sigma = 8$–$13\,\%$) synthesized according to the procedure described in the Experimental Section. These NPs were dispersed in toluene and stabilized by weakly bound surfactants (oleylamine and oleic acid). The "reactions" between the particles were initiated by the addition of 1,4-benzenedimethanethiol cross-linker (see Section 1 in the Supporting Information for other types of cross-linkers studied), which attached selectively to the gold portions of the particles and mediated their aggregation. Because of the presence of large, "unreactive" Fe_3O_4 domains surrounding the cross-linked Au parts, however, the particles did not aggregate completely into a bulk precipitate but instead formed soluble, finite-sized clusters. The number of particles, n, in these clusters varied from two to more than five (Figure 2). We observed that 1) n increased with increasing concentration of the dithiol cross-linkers, C, which, as we will see shortly, can be related to the effective strength of dithiol-mediated Au–Au binding ("bond strength"); and 2) n decreased with increasing value of the steric hindrance parameter, $s = R_2/R_1$, which measures the bulkiness of the Fe_3O_4 domains relative to the Au domains (cf. Figure 1b). The images of typical clusters are shown in Figure 2, and their fractions as a function of C and s are quantified in Figure 3. Although for all conditions studied, the NPs gave a mixture of different types of clusters, the "selectivity" (i.e., percentage of

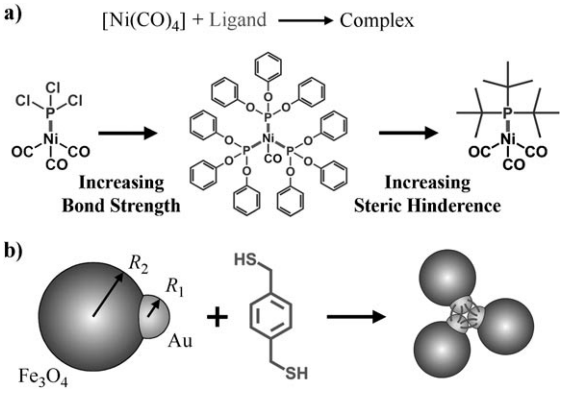

Figure 1. a) A chemical analogy: the effects of bond strength and steric hindrance on the replacement of CO from $[Ni(CO)_4]$ with various phosphorus-based ligands.[24] The average number of bound ligands increases with increasing bond strength for ligands with similar steric effects (as characterized by the ligand cone angle θ; e.g., $\theta(PCl_3) \approx 124°$ and $\theta[P(OC_6H_5)_3] \approx 128°$). For similar bond strengths, the number of bound ligands decreases with increasing steric effects (here, $\theta[P(OC_6H_5)_3] \approx 128°$ vs. $\theta[P(t\mathrm{Bu})_3] \approx 182°$). b) Scheme of the composite Au/Fe_3O_4 NPs and 1,4-benzenedimethanethiol molecules used to "react" the individual particles into nanoclusters (here, a trimer, $n = 3$).

[*] Dr. Y. Wei, Dr. K. J. M. Bishop, J. Kim, S. Soh, Prof. B. A. Grzybowski
Department of Chemistry, Department of Chemical and Biological Engineering, Northwestern University
2145 Sheridan Road, Evanston, IL 60208 (USA)
E-mail: grzybor@northwestern.edu
Homepage: http://dysa.northwestern.edu

[**] This work was supported by a Pew Scholarship, a Sloan Fellowship, and by a grant from the Camille & Henry Dreyfus Foundation (to B.A.G.). K.J.M.B. was supported by an NSF graduate fellowship.

Supporting information for this article is available on the WWW under http://dx.doi.org/10.1002/anie.200903864.

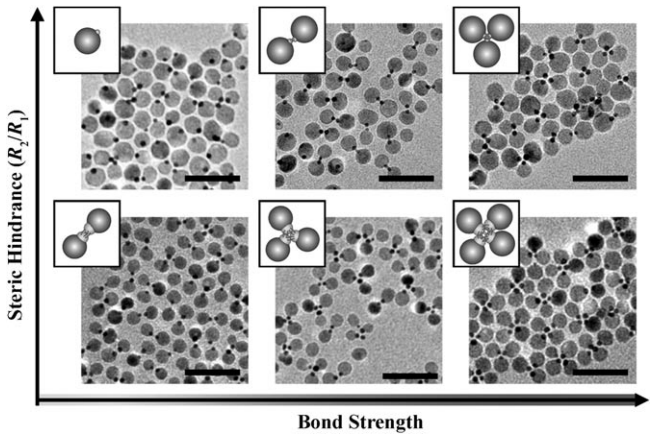

Figure 2. TEM images of nanoclusters obtained for different "bond strengths" (determined by the dithiol concentration) and "steric hindrance" (quantified by the ratio, $s = R_2/R_1$). The insets provide a schematic illustration of the most probable NP cluster. The images correspond to dithiol concentrations of 0.3 μM, 5 μM, 500 μM (left to right) and steric parameters, $s = R_2/R_1$, of 2.9 and 3.8 (bottom and top, respectively). All scale bars are 50 nm.

the major product in the mixture) of these nanoscale "reactions" could be as high as ≈75% and comparable to typical yields of organic reactions.

While the bond strength and steric hindrance analogies with molecular systems (cf. Figure 1a) are attractive, they need to be substantiated by more rigorous thermodynamic considerations. We first consider the relationship between the dithiol concentration and the effective strength of binding between Au domains. In dilute solution, the chemical potential of the dithiols is given by $\mu_S = \mu_S^0 + kT \ln x$, where μ_S^0 is the standard chemical potential, kT is the thermal energy, $x = C/C_S$ is the mole fraction of dithiols in solution, and C_S is the solvent concentration (e.g., 7.7 M for hexane). For dithiols adsorbed onto a *single* gold surface, the chemical potential, μ_1, may be approximated by the Langmuir-type isotherm, where θ_1 is the fractional coverage of dithiol adsorbed on the surface, $\mu_1 = \mu_1^0 + kT \ln[\theta_1/(1-\theta_1)]$.

At equilibrium, the chemical potentials for free and adsorbed dithiols are equal, such that $\theta_1^{eq}/x(1-\theta_1^{eq}) = \exp(-\Delta\mu_{s1}^0/kT)$ where $\mu_{s1}^0 = \mu_1^0 - \mu_S^0$ is the energy of adsorption—roughly equal to the strength of one thiol–gold bond, $\mu_{s1}^0 \approx -3.4 \times 10^{-20}$ J.[26] Furthermore, the total free energy per unit area, f_1, of this system may be estimated by thermodynamic integration from the reference state ($\theta = 0$) to the equilibrium state ($\theta = \theta_{eq}$) [Eq. (1)], where Γ

$$f_1 = \Gamma \int_0^{\theta_1^{eq}} (\mu_S - \mu_1)\mathrm{d}\theta = -\Gamma kT \ln(1-\theta_1^{eq}) \quad (1)$$

$\approx 4.7\ \mathrm{nm}^{-2}$ is the maximum surface density of dithiols adsorbed onto the gold surface.[27] With these preliminaries, one can calculate the free energy of dithiol cross-linking of two gold domains. Assuming that all adsorbed dithiols bind to both surfaces with fractional coverage θ_2, the chemical potential, μ_2, of the cross-linking molecules joining the two surfaces can be expressed as $\mu_2 = \mu_2^0 + kT \ln[\theta_2/(1-\theta_2)]$, and the corresponding free energy of formation (per unit area) for two cross-linked surfaces can be approximated as $f_2 = \Gamma kT \ln(1-\theta_2^{eq})$. The free energy of the cross-linking interaction per unit area, Δf, may then be expressed as Equation (2), where the free energy of divalent binding by a

$$\Delta f = 2f_1 - f_2 = \Gamma kT \ln\left(\frac{[1 + x\exp(-\Delta\mu_{s1}^0/kT)]^2}{1 + x\exp(-\Delta\mu_{s2}^0/kT)}\right) \quad (2)$$

cross-linking ligand, $\Delta\mu_{s2}^0$, is roughly two times greater than that of monovalent binding, $\Delta\mu_{s1}^0$, such that $\Delta\mu_{s2}^0 \approx 2\Delta\mu_{s1}^0$. With this substitution, multiplication by the effective area of contact between two spherical Au domains, $A_{eff} = 2\pi R_1\delta$ ($\delta \approx 1$ Å is a characteristic length scale of the cross-linking interaction[28]), gives the energy of cross-linking two Au domains of radii R_1 ("bond strength") [Eq. (3)]. This approx-

$$\varepsilon = (2\pi R_1\delta)\Delta f \approx -(2\pi R_1\delta)\Gamma kT \ln(1 + x\exp(-2\Delta\mu_{s1}^0/kT) \quad (3)$$

imate form is valid for $x < \exp(\Delta\mu_{s1}^0/kT)$, which is satisfied for the experimental conditions described here; that is, for $\Delta\mu_{s1}^0 \approx -8.5\,kT$ at room temperature[26] and $x = 10^{-9}$ to 10^{-5}.

We make the following observations about this expression. First, the "bond strength" is always favorable, $\varepsilon < 0$, and its magnitude increases not only with the radii of the contacting domains but also with the concentration of dithiols (since $x \propto C$). The concentration dependence predicted by Equation (3) applies to other types of molecules that can be used to link nanoparticles, notably DNA-based linkers (see Section 2 in the Supporting Information for a discussion of the model in the context of DNA cross-linking[25]). Second, the strength of this interaction is sufficiently large (e.g., $\varepsilon \approx -30\,kT$ for $R_1 = 2$ nm and $x = 10^{-5}$) relative to the thermal energy (kT) to induce NP aggregation from solution. Third, while Equations (2) and (3) are *free* energy differences accounting for the entropic contributions of the dithiols to the cross-linking interaction, they do not account for the entropy changes of the NPs themselves upon cluster formation. With respect to the NPs, Equation (3) therefore represents a *potential* energy of interaction and describes only the energetic contribution to the total free energy, ΔF_n, of forming an n-sized cluster.

This total free energy of NP cluster formation consists of both favorable energetic contributions due to cross-linking interactions as well as unfavorable entropic contributions associated with the NPs' loss of translational/rotational degrees of freedom upon aggregation from solution. The fact that the sizes of the NP clusters depend on the strength of the cross-linking "bonds" (i.e., on the dithiol concentration; Figure 3a,b) suggests that both the energy and the entropy of cluster formation contribute significantly to ΔF_n, which ultimately determines which cluster size is favored at equilibrium. Alternatively, if cluster formation were governed solely by the energetic contributions, there would be no such dependence on the dithiol concentration, and only minimal energy clusters would be observed. The free energy is of the form, $\Delta F_n \approx N_n\varepsilon + T\Delta S_n$, in which N_n is the number of cross-linking "bonds" in an n-sized cluster, and ΔS_n is the entropy of

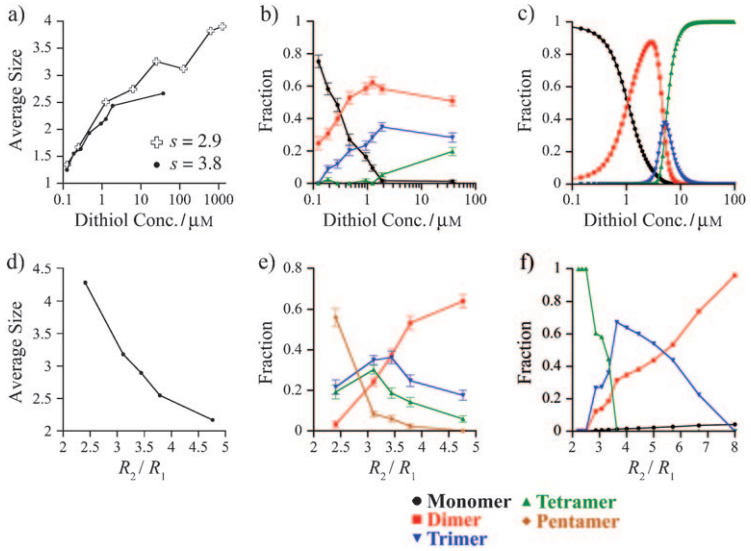

Figure 3. a–c) Cluster size as a function of the dithiol concentration, *C*, for Fe_3O_4/Au NPs with steric parameters, $s = R_2/R_1 = 2.9$ and 3.8. a) The average cluster size increases with increasing *C* due to increasingly stronger crosslinking interactions between the gold domains. Experimentally observed (b) and theoretically predicted (c) fractions of NPs comprising monomers, dimers, trimers, and tetramers as a function of the dithiol concentration for $R_2/R_1 = 3.8$; see colored symbols defined in the figure. Clusters statistics were obtained from TEM images; details of the model calculations and the parameters used can be found in the Supporting Information. d–f) Cluster size as a function of the steric parameter R_2/R_1 for Fe_3O_4/Au NPs assembled at dithiol concentrations of 13 μM. d) The average size of the "nanomolecules" decreases with increasing steric hindrance, as characterized by the steric parameter R_2/R_1. Experimentally observed (e) and theoretically predicted (f) fractions of NPs comprising monomers, dimers, trimers, tetramers, and pentamers as function of R_2/R_1; see colored symbols defined in the figure. Error bars are based on the statistics described in detail in Section 7 of the Supporting Information.

forming such a cluster. Stronger cross-linking interactions (increasing $|\varepsilon|$) results in the formation of larger clusters because NPs form more Au–Au "bonds" (larger N_n) in larger clusters than in smaller ones (e.g., one bond for dimers vs. three bonds for trimers). Consequently, the free energy of forming larger clusters decreases more rapidly with ε than that of smaller clusters, and larger clusters become increasingly favorable as the concentration of dithiol increases.

The fact that the sizes of the clusters are limited (even at the highest dithiol concentrations) and that for a given concentration of dithiols the cluster sizes decrease with increasing $s = R_2/R_1$ is a result of the presence of Fe_3O_4 domains surrounding the Au–Au "bonds" (Figure 3d,e). These domains introduce steric hindrance analogous to that in molecular systems and influence both the energy and the entropy of cluster formation (in chemistry these two contributions are often termed "steric strain" and "steric hindrance", respectively[29,30]). Specifically, the energy of cluster formation (approximately $N_n\varepsilon$) depends on the steric parameter through the number of cross-linking "bonds", N_n, which is determined by the geometry of the particles. On the other hand, increasing the steric parameter increases the unfavorable entropy of cluster formation (ΔS_n) by decreasing the translational and rotational freedom of NPs within the cluster. For increasingly bulky Fe_3O_4 domains, the NPs have fewer possible configurations (i.e., smaller accessible phase space) within the cross-linked aggregates and therefore lower entropy.

To explore the effects of bond strength and steric hindrance in more quantitative detail, we used the methods of statistical mechanics to calculate the free energies of cluster formation and the equilibrium cluster statistics. Accounting for the energy of cross-linking, ε, and for the van der Waals interactions between the particles (magnetic interactions were found to be negligible; cf. Section 4 in the Supporting Information), we used the so-called statistical theory of physical clusters to calculate,[31] by means of Monte Carlo integration, the canonical partition functions, Q_n, of *n*-sized clusters (see Section 5 in the Supporting Information). These functions were then related to the free energies—accounting for both "bonding" energies as well as entropic effects—of cluster formation, $\Delta F_n = k_B T \ln(Q_1^n/Q_n)$, and could be used to model the distributions of cluster sizes (i.e., to the fractions of monomers, dimers, etc.) by solving the set of algebraic equations, $N_1^n/N_n = Q_1^n/Q_n$, with the conservation equation, $N_{tot} = \sum_n nN_n$.

Figure 3c,f show that the cluster statistics predicted by this model are in qualitative agreement with the experimental trends from Figure 3b,e. For high dithiol concentrations (corresponding to strong "bonds"), however, the theoretical dependencies differ even qualitatively from the experimental results, likely because of polydispersity in the size and geometry of the Fe_3O_4/Au NPs. In this limit, cluster formation should be governed entirely by energetic effects (i.e., entropic effects are negligible), and the clusters sizes should be insensitive to further increases in the dithiol concentration (as observed in experiments). Under these conditions, the model—assuming monodisperse particles—predicts the formation of a single cluster size corresponding to the minimum potential energy for a given geometry/size of the constituent particles. In contrast, experiments at high cross-linker concentrations reveal an "asymptotic" distribution of cluster sizes (cf. Figure 3b) owing to the polydispersity of the NPs. Inspection of individual clusters using high-resolution TEM demonstrate that smaller clusters comprise NPs with steric parameters, R_2/R_1, greater than the average value; meanwhile, the largest clusters incorporate NPs with the smallest values of the ratio R_2/R_1. Thus, it is likely that these clusters represent the minimal energy configuration for the solution of *polydisperse* NPs. We note that in the regime of small bond strength, NP polydispersity is less important as evidenced by the better agreement between the model (monodisperse) and experiments (somewhat polydisperse).

In conclusion, we have demonstrated that the chemical concepts of bond strength and steric hindrance can be extended to and applied at the nanoscale to "react" composite NPs into clusters of symmetries lower than those of the constituent pieces. This experimental approach and the

theoretical model that supports it are of general nature and could be applied for various asymmetric components, for which attractive interactions and steric/entropic repulsions can be tuned controllably. Improving the yields of specific "nanomolecules" will require either the use of more monodisperse components or—continuing the chemical analogy—subsequent purification of the "nanomolecules" through magnetic[32] or gel electrophoretic[33] separation techniques.

Experimental Section

Synthesis of heterodimeric Fe_3O_4/Au nanoparticles: In a typical procedure, 6 mmol oleylamine (OAM), 6 mmol oleic acid (OA), 10 mmol 1,2-tetradecanediol, and 22 mL 1-octadecene (ODE) were added to a three-neck flask under argon and degassed completely. The reaction mixture was heated to 120 °C under argon before 2 mmol $[Fe(CO)_5]$ was injected at the same temperature. The reaction mixture was stirred for 5 min before a solution of 0.1 mmol $HAuCl_4 \cdot 3H_2O$ in 3 mL ODE was injected. The reaction solution was then heated slowly to reflux (at 1 °C min^{-1}) and kept at reflux for 1 h. After cooling to room temperature, the reaction solution was opened to air and stirred for 1 h. The resulting NPs were precipitated by addition of acetone and centrifuged for 10 min at 1500 g, after which they were redispersed in 20 mL toluene containing 50 mM OAM and 50 mM OA. The toluene solution was centrifuged for 30 s, and the sedimented precipitate was removed. The remaining dark brown-red supernatant was precipitated by addition of 6 mL ethanol followed by centrifugation, and the resulting precipitate was redispersed in 10 mL toluene with 100 μL OA and 100 μL OAM.

This procedure resulted in the formation of stable, peanut-shaped NPs with 11.8 nm Fe_3O_4 domains and 3.8 nm Au domains. Other sizes were obtained by varying the surfactant concentration, Fe/Au ratio, and/or the injection temperature. Specifically, the size of the Fe_3O_4 domain was tuned by varying the concentration of surfactants and the Fe/Au ratio: higher surfactant concentrations or lower Fe/Au ratios resulted in smaller Fe_3O_4 domains. The size of the Au domain was tuned by changing the concentration of surfactants or the temperature at which $HAuCl_4 \cdot 3H_2O$ was injected: higher surfactant concentrations or lower injection temperatures resulted in smaller Au domains.

Preparation of "nanomolecules" from Fe_3O_4/Au NPs: In a typical procedure for preparing dimeric clusters, 100 μL toluene solution of (14.4 nm Fe_3O_4)/(3.0 nm Au) composite NPs was first diluted with 3.9 mL hexane before 500 μL of a 1,4-benzenedimethanethiol solution (12.5 μM in toluene) was added, and the reaction mixtue was then sonicating for 10 to 30 min. Other "nanomolecules" were prepared using the same dilutions/concentrations but with Fe_3O_4/Au NPs characterized by different R_1/R_2 ratios and/or by adding different amounts of dithiol cross-linker to the NP solutions.

Received: July 15, 2009
Revised: August 14, 2009
Published online: November 7, 2009

Keywords: bond strength · dimers · nanoparticles · steric hindrance

[1] G. M. Whitesides, B. Grzybowski, *Science* **2002**, *295*, 2418.
[2] M. Fialkowski, K. J. M. Bishop, R. Klajn, S. K. Smoukov, C. J. Campbell, B. A. Grzybowski, *J. Phys. Chem. B* **2006**, *110*, 2482.
[3] a) A. M. Kalsin, M. Fialkowski, M. Paszewski, S. K. Smoukov, K. J. M. Bishop, B. A. Grzybowski, *Science* **2006**, *312*, 420; b) K. J. M. Bishop, C. E. Wilmer, S. Soh, B. A. Grzybowski, *Small* **2009**, *5*, 1600.
[4] C. Desvaux, et al., *Nat. Mater.* **2005**, *4*, 750.
[5] Z. L. Zhang, S. C. Glotzer, *Nano Lett.* **2004**, *4*, 1407.
[6] F. Dmitrii, F. Rosei, *Angew. Chem.* **2007**, *119*, 6112; *Angew. Chem. Int. Ed.* **2007**, *46*, 6006.
[7] P. C. Ohara, D. V. Leff, J. R. Heath, W. M. Gelbart, *Phys. Rev. Lett.* **1995**, *75*, 3466.
[8] R. Klajn, K. J. M. Bishop, B. A. Grzybowski, *Proc. Natl. Acad. Sci. USA* **2007**, *104*, 10305.
[9] L. Han, et al., *Chem. Mater.* **2003**, *15*, 29.
[10] R. Klajn, K. J. M. Bishop, M. Fialkowski, M. Paszewski, C. J. Campbell, T. P. Gray, B. A. Graybowski, *Science* **2007**, *316*, 261.
[11] E. V. Shevchenko, D. V. Talapin, N. A. Kotov, S. O'Brien, C. B. Murray, *Nature* **2006**, *439*, 55.
[12] A. P. Alivisatos, et al., *Nature* **1996**, *382*, 609.
[13] C. A. Mirkin, R. L. Letsinger, R. C. Mucic, J. J. Storhoff, *Nature* **1996**, *382*, 607.
[14] S. Y. Park, et al., *Nature* **2008**, *451*, 553.
[15] M. H. Hu, L. P. Qian, R. P. Brinas, E. S. Lymar, J. F. Hainfeld, *Angew. Chem.* **2007**, *119*, 5203; *Angew. Chem. Int. Ed.* **2007**, *46*, 5111.
[16] F. Patolsky, Y. Weizmann, I. Willner, *Nat. Mater.* **2004**, *3*, 692.
[17] J. P. Novak, D. L. Feldheim, *J. Am. Chem. Soc.* **2000**, *122*, 3979.
[18] G. A. DeVries, et al., *Science* **2007**, *315*, 358.
[19] R. Sardar, J. S. Shumaker-Parry, *Nano Lett.* **2008**, *8*, 731.
[20] K. K. Caswell, J. N. Wilson, U. H. F. Bunz, C. J. Murphy, *J. Am. Chem. Soc.* **2003**, *125*, 13914.
[21] S. T. Shibu Joseph, B. I. Ipe, P. Pramod, K. G. Thomas, *J. Phys. Chem. B* **2006**, *110*, 150.
[22] Y. H. Wei, R. Klajn, A. O. Pinchuk, B. A. Grzybowski, *Small* **2008**, *4*, 1635.
[23] H. Yu, et al., *Nano Lett.* **2005**, *5*, 379.
[24] C. A. Tolman, *Chem. Rev.* **1977**, *77*, 313.
[25] P. L. Biancaniello, A. J. Kim, J. C. Crocker, *Phys. Rev. Lett.* **2005**, *94*, 058302.
[26] D. S. Karpovich, G. J. Blanchard, *Langmuir* **1994**, *10*, 3315.
[27] D. V. Leff, P. C. Ohara, J. R. Heath, W. M. Gelbart, *J. Phys. Chem.* **1995**, *99*, 7036.
[28] J. N. Israelachvili, *Intermolecular and Surface Forces*, 2nd ed., Academic Press, New York, **1991**.
[29] R. J. Taft, *J. Am. Chem. Soc.* **1953**, *75*, 4538.
[30] R. J. Taft, *J. Am. Chem. Soc.* **1953**, *75*, 4534.
[31] T. L. Hill, Statistical Mechanics: Principles and Selected Applications, Dover, New York, **1987**.
[32] C. T. Yavuz, et al., *Science* **2006**, *314*, 964.
[33] M. Hanauer, S. Pierrat, I. Zins, A. Lotz, C. Sonnichsen, *Nano Lett.* **2007**, *7*, 2881.

